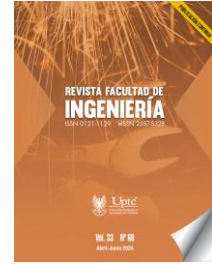




Revista Facultad de Ingeniería

Journal Homepage: <https://revistas.uptc.edu.co/index.php/ingenieria>



# Positive B-splines used as Mappings in the Probabilistic Quantizer

Juan-Pablo Hoyos-Sánchez<sup>1</sup>  

Pablo-Emilio Jojoa<sup>2</sup>  

**Received:** March 21, 2023

**Accepted:** May 30, 2024

**Published:** June 5, 2024

**Citation:** J.-P. Hoyos-Sánchez, P.-E. Jojoa, "Positive B-splines used as Mappings in the Probabilistic Quantizer," *Revista Facultad de Ingeniería*, vol. 33, no. 68, e17387, 2024. <https://doi.org/10.19053/01211129.v33.n68.2024.17387>

## Abstract

A Dithered quantizer consists of an external signal called Dither added to the input signal prior to quantization to control the statistical properties of the quantization error. In the framework known as Quantum Signal Processing (QSP) an equivalent quantizer was developed, called probabilistic quantizer, which is able to generate a Dither signal with an arbitrary joint probability distribution. This paper demonstrates how positive B-spline functions can be used as a mapping in the probabilistic quantizer and the mathematical advantages to perform their analysis. In addition, we established a relation between the order of the B-spline and the rendering of conditional moments of the error. Experimental results show that the proposed approach performs on par with Dither quantizer, and its implementation is easier.

<sup>1</sup> Ph. D. Universidad Nacional de Colombia (La Paz-Cesar, Colombia). [jhoyoss@unal.edu.co](mailto:jhoyoss@unal.edu.co)

<sup>2</sup> Ph. D. Universidad del Cauca (Popayán-Cauca, Colombia). [pjojoa@unicauca.edu.co](mailto:pjojoa@unicauca.edu.co)



**Keywords:** B-spline; conditional moments; Dither quantizer; probabilistic quantizer; quantum signal processing.

### **B-Splines positivas usadas como mapeos en el cuantificador probabilístico**

#### **Resumen**

Un Cuantificador Dither consiste en una señal externa denominada Dither que se añade a la señal de entrada antes de la cuantización para controlar las propiedades estadísticas del error de cuantización. En el marco conocido como Procesamiento Cuántico de Señales (QSP por sus siglas en inglés), se desarrolló un cuantificador equivalente denominado cuantificador probabilístico, el cual es capaz de generar una señal Dither con una distribución de probabilidad conjunta arbitraria. Este trabajo demuestra cómo las funciones B-spline positivas pueden utilizarse como mapeo en el cuantificador probabilístico y las ventajas matemáticas para realizar su análisis. Además, establecemos una relación entre el orden de la B-spline y la representación de los momentos condicionales del error. Los resultados experimentales muestran que el enfoque propuesto ofrece un rendimiento a la par que el cuantificador Dither y su implementación es más fácil.

**Palabras clave:** B-spline; cuantificador Dither; cuantificador probabilístico; momentos condicionales; procesamiento cuántico de señales.

### **B-Splines positivos usados como mapeamentos no cuantificador probabilístico**

#### **Resumo**

Um Dither Quantizer consiste em um sinal externo chamado Dither que é adicionado ao sinal de entrada antes da quantização para controlar as propriedades estatísticas do erro de quantização. Na estrutura conhecida como Processamento Quântico de Sinais (QSP), foi desenvolvido um quantizador equivalente denominado quantizador probabilístico, que é capaz de gerar um sinal Dither com uma distribuição de probabilidade conjunta arbitrária. Este trabalho demonstra como funções B-spline positivas podem ser utilizadas como mapeamento no quantizador probabilístico e as vantagens matemáticas para realizar sua análise. Além disso, estabelecemos uma relação entre a ordem do B-spline e a representação dos momentos condicionais do erro. Os resultados experimentais mostram que a abordagem proposta oferece desempenho comparável ao quantizador Dither e sua implementação é mais fácil.

**Palavras-chave:** B-spline; Quantificador de pontilhamento; quantificador probabilístico; momentos condicionais; processamento quântico de sinais.

## I. INTRODUCTION

The conversion of a signal from analog to digital generally comprises two processes: sampling, which converts a signal (a function of time) into a discrete-time signal (a sequence of real numbers); and quantization of the amplitude values, a nonlinear process that assigns a binary code to each signal sample [1]. In quantization designs, under certain conditions (e.g., Quantization Theorem I and II in [2]), from a point of view of moments, the quantization error can be modeled as an additive random process, independent of the input signal and distributed uniformly [2]. This linear behavior is highly desirable in many circumstances [2]-[5].

However, if the input has magnitude values comparable to the quantizer step, the error signal  $\epsilon$  cannot be modeled as an additive random process due to its strongly dependence on the input [6]. The most common approach to solve it has been the use of Dithered quantizer because it satisfies the QT II, thus controlling the statistical properties of the quantization error and their relationship to the input signal of the system by adding a random signal, called the Dither signal, to the input signal before quantization [3], [7]. It is widely employed, for example in audio and image processing applications to reduce perceptual artifacts [8]; in ADCs to improve the resolution [9], [10] and security [11]; in sigma-delta digital modulators [12]–[14]; in Watermark to hide data [15] in Light detection [16,17]; and in finite frames [18]–[20]. Recently, Dither quantization has been used in the quantization of random linear mapping outputs, particularly in compressed sensing [21]-[23] and in spatial Dithering for graph signal to find statistically good sampling sets [24].

Despite the benefits of the Dither quantizer, one of its disadvantages is computational complexity to generate random processes (Dither signals) subject to an arbitrary joint probability distribution [7] because, in practice, they are commonly generated as a combination of  $n$  uniform independent, identically distributed, random variables. Sanyal and Sun [25] proposed a new method for adding Dither signals to vector quantizers, which achieves a better mismatch shaping performance with low hardware usage compared to existing Dither techniques. Akyol and Rose [5] developed a constrained Dither quantizer that outperforms the conventional Dither quantizer with similar complexity. In [26], it was demonstrated how the resolution of a uniform quantizer increases by using a deterministic Dither signal, and in [27], the authors designed an alternative Dithering scheme that replaced the Dithering addition by an orthogonal transformation.

Given this limitation, a new framework called Quantum Signal Processing (QSP) [28] that is aimed at developing new or modifying existing signal processing algorithms by borrowing

from the principles of quantum mechanics and some of its interesting axioms and constraints, presents a probabilistic quantizer that has a direct relationship with the Dither quantizer and can generate a Dither signal with an arbitrary joint probability distribution using only a uniform random variable as input. Therefore, it reduces the computational complexity; however, it needs a mapping function with specific characteristics in time and frequency domain.

This paper shows that the positive B-splines satisfy the conditions to be a mapping for the uniform probabilistic quantizer and establishes a relation between the order of B-spline and the rendering of conditional moments of the error. One advantage of using B-splines is that they can be explicitly characterized, thus, their analysis is easier by eliminating convergence issues. Finally, we verify the result through numerical simulations and show that the proposed approach performs on par with Dither quantizer, but only requires the generation of a random variable.

## II. METHODOLOGY

In value amplitude quantization, a binary code is assigned to each signal sample, then the quantization process performs a mapping from the analog world to the digital one. It is necessary to acknowledge the inevitable degradation suffered by the signal, which is characteristic of the quantization process. More precisely, the quantizer input is a sequence that must belong to the space of sequences of finite energy ( $\ell^2$ ) to bring stability to the quantification process. For each input value  $x_n$ , there will be a corresponding quantized value given by  $y_n = Q(x_n)$ , where the quantizer  $Q$  selects one of the quantization levels according to a defined rule, and the difference between each level is equal to  $\Delta$ . In the operation of the QSP quantizer, the scalar quantizer defined as:

$$Q(x) = \Delta \left\lfloor \frac{x}{\Delta} + \frac{1}{2} \right\rfloor \quad (1)$$

It was taken as a base, where the operator  $\lfloor \cdot \rfloor$  returns the largest integer, which is less than or equal to its argument. The  $\Delta$  step is commonly referred to as the least significant bit (LSB) since a change in the input signal of one step at the most will generate a change in the LSB of the binary code of the output [2]. The transfer function of the scalar quantizer is shown in Figure 1.

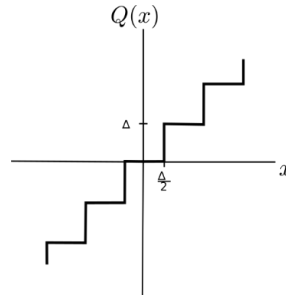


Fig. 1. Characteristic Transfer function of a uniform quantizer.

**A. Probabilistic Quantizer**

The QSP probabilistic quantizer in the vector space  $\mathbb{R}$  is shown in Figure 2 [28].

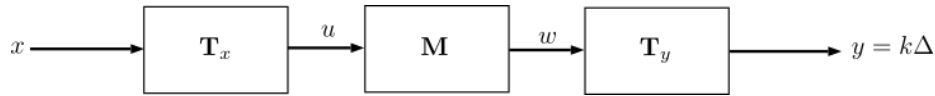


Fig. 2. Description of the Probabilistic Quantizer.

To ensure stability in the quantification process, an input transformation  $T_x: \mathbb{R} \rightarrow \ell_2$  is applied, mapping the input to the space of sequences with finite energy. To obtain the quantized value, a transformation  $T_y: \ell_2 \rightarrow \mathbb{R}$  is defined, such that  $T_y = y = k\Delta$ . The QSP measurement, denoted as  $M$  is constructed on  $\ell_2$ , and employs a probabilistic assignment rule  $f$  to assign a corresponding output value  $w$  to each input value  $u$ . This quantizer is called QSP Quantizer with mapping  $f$ . Then, using this probabilistic mapping  $f$ , the quantization process can be expressed as follows:

$$Q_M(x) = k\Delta, \quad \text{with } k = f(x) \quad (2)$$

where  $f$  depends on the input  $x$  through the numbers  $\{x - k\Delta\}$ . For example, the uniform quantizer is obtained when  $f(x) = \arg \min_{i \in \mathcal{K}} |x - i\Delta|$ , then different mappings result in new and interesting quantizers.

When developing the probabilistic quantizer, we choose a probabilistic mapping  $f: \mathbb{R} \times W \rightarrow \mathbb{Z}$  where  $\{W = \mathbb{Z}\}$  represents the sample space of a discrete auxiliary variable  $w$  with alphabet  $\mathbb{Z}$ . As such, the variable  $w$  can only take values  $w_k = k \in \mathbb{Z}$  with probability  $p_k = h(x - k\Delta)$  for certain function  $h(x)$ . The mapping assigns an index  $k$  for each input through  $f(x, k) = k$ , and the output of the quantizer is

$$y = k\Delta, \text{ with probability } p_k = h(x - k\Delta) \quad (3)$$

This quantizer will be referred to as a Probabilistic quantizer with mapping  $h(x)$ . The mapping should fulfill the following condition in the time domain [28]

$$h(x - i\Delta) \geq 0 \quad \text{and} \quad \sum_{i=-\infty}^{+\infty} h(x - i\Delta) = 1. \quad (4)$$

while in the frequency domain, the condition of the mapping is given by

$$H\left(\frac{2\pi}{\Delta}i\right) = \Delta\delta[i], \quad i \in \mathbb{Z} \quad (5)$$

where  $H(\omega)$  represents the Fourier transform of  $h(x)$ , and  $\delta[i]$  is the Dirac delta function.

### B. Relationship Between Probabilistic and Non-subtractive Dithered (NSD) Quantizers

When the characteristic function of the input signal  $x$  is bandlimited, the moments of  $x$  can be obtained from the moments of  $y$  if the frequency of quantization ( $2\pi/\Delta$ ) is higher than the highest frequency component of the characteristic function (CF) of  $x$ . But, when  $x$  is not bandlimited, another method must be used. One option is non-subtractive Dithered quantizer (NSD). It consists in adding an independent signal  $v$  (Dither) to signal  $x$  to control the bandwidth of the quantizer input signal characteristic function  $x + v$ , and satisfies the Widrow quantizing theorems [2, QT I-II], as shown in Figure 3. Moreover, NSD systems are designed to control the statistical characteristics of the error  $\epsilon = y - x$  [6], [7].

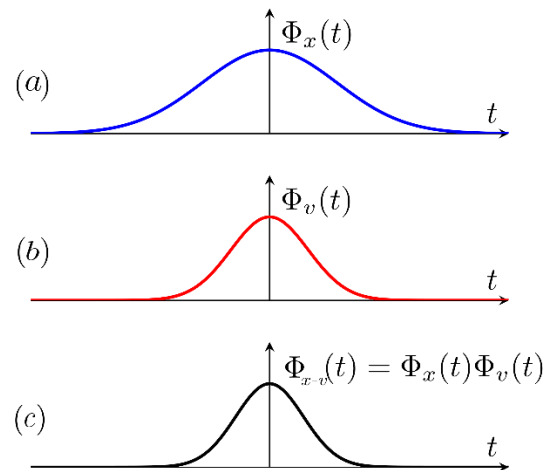


**Fig. 3.** Band limitation of characteristic function of quantizer input signal  $w$  resulting from Dithering with a bandlimited independent Dither signal  $v$ . (a) CF of  $x$  no bandlimited, (b) CF of Dither signal  $v$  bandlimited, (c) CF of quantizer input  $x + v$  bandlimited.

The Dither signal is assumed to be stationary and statistically independent of input  $x$  and serves as lowpass antialias filtering for  $\Phi_x(t)$ . Figure 4 shows a block diagram of a memoryless or non-subtractive Dithered quantizer.

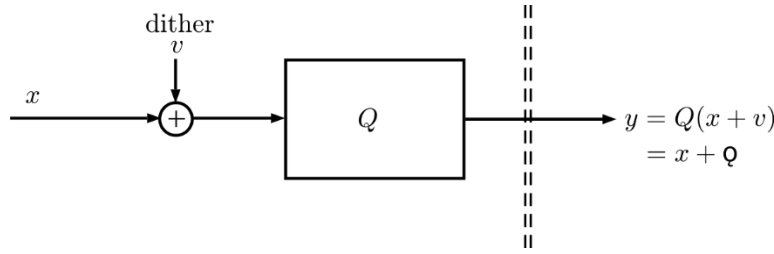


Fig. 4. Non-subtractive Dithered quantization (NSD).

The probability of the NSD quantizer output  $y = Q(x + v)$  is defined as [28]

$$p_k(y = k\Delta) = \mathbf{1}_\Delta(x - k\Delta) * f_v(-x) \quad (6)$$

where  $*$  denotes the convolution operator,  $f_v$  is the Probability Density Function (PDF) of the Dither signal, and

$$\mathbf{1}_\Delta = \begin{cases} 1 & -\Delta/2 \leq x \leq \Delta/2 \\ 0 & \text{otherwise} \end{cases} \quad (7)$$

Now, comparing  $p_k(y)$  from (6) with (3), the mapping is equivalent to

$$h(x) = \mathbf{1}_\Delta(x) * f_v(-x) \quad (8)$$

and in the frequency domain is

$$H(\omega) = \Delta \text{sinc}\left(\frac{\Delta\omega}{2}\right) F_v(-\omega) \quad (9)$$

where  $F_v$  is the Fourier transform of  $f_v$ , and  $\text{sinc}(x) = \sin(x)/x$ . To sum up, a NSD quantizer with a Dither signal with PDF  $f_v(v)$  is equivalent to a probabilistic quantizer with mapping  $h(x)$ . And the necessary relationship between  $h(x)$  and  $f_v(v)$  in the time domain is defined by ([eq\_relation]) and its equivalent in the frequency domain by (9).

### C. B-Spline Function as Mapping $h(x)$

Although it is possible to find mappings that satisfy the previous conditions, the main drawback is to achieve that certain moments of the error can be independent of the input. This section presents a family of splines that satisfies these requirements. A basic spline or B-spline of degree  $p$  is a polynomial function constrained to be Hölder continuous of order  $p$  [29]. The B-spline of order  $p = 0$  is the well known Haar scaling, defined by

$$\beta_{Haar}^0(t) = u(t) - u(t - 1) \quad (10)$$

where  $u(t)$  is the Heaviside step function. It is of our interest to include the  $\Delta$  step, then the B-spline of order  $p = 0$  is reformulated as

$$\beta_+^0(t) = u\left(\frac{t}{\Delta}\right) - u\left(\frac{t}{\Delta} - 1\right) \quad (11)$$

with the Fourier transform given by

$$B_+^0(\omega) = \frac{1 - e^{-j\omega\Delta}}{j\omega\Delta} \quad (12)$$

The basic spline of order  $p$  is defined by  $p$  convolutions of  $\beta^0$ :

$$\beta_+^p = \beta_+^{p-1} * \beta_+^0 \tag{13}$$

and using the Fourier properties, its transform is given by:

$$B_+^p(\omega) = \left( \frac{1 - e^{-j\omega\Delta}}{j\omega\Delta} \right)^{p+1} \tag{14}$$

when the degree tends to infinity, the B-splines converge to the *sinc* wavelet [30]. Furthermore, B-splines produce scaling or wavelet functions with an explicit analytical form [29 -31], and they can be implemented by finite or infinite impulse response filter [32],[33]. To have more freedom in the selection of the mapping, we use the extension of B-spline with non-integer order, called fractional B-splines [34]:

$$\beta_+^p(t) = \frac{1}{\Gamma(p+1)} \sum_{i \geq 0} (-1)^i \binom{p+1}{i} \left( \frac{t}{\Delta} - i \right)_+^p \tag{15}$$

These splines have compact support only when  $p$  is an integer, resulting into basic splines [34]. Because the support belongs to  $\mathbb{R}_+$ , these splines are called causal. In this paper we are only interested in positive and centered B-splines because we need to represent a probability density function of a random variable or Dither. The centered B-spline and its Fourier transform are expressed as:

$$\beta_0^p = \beta_+^p(t + \tau) \xleftrightarrow{\mathcal{F}} B_0^p(\omega) = e^{-j\omega\tau} B_+^p(\omega) \tag{16}$$

where  $\tau = \Delta(p + 1)/2$  is the shift necessary to center the spline. We focus on fractional centered positive B-splines, orders  $p = 0.1$  and  $p \geq 2$  as show in Figure 5.

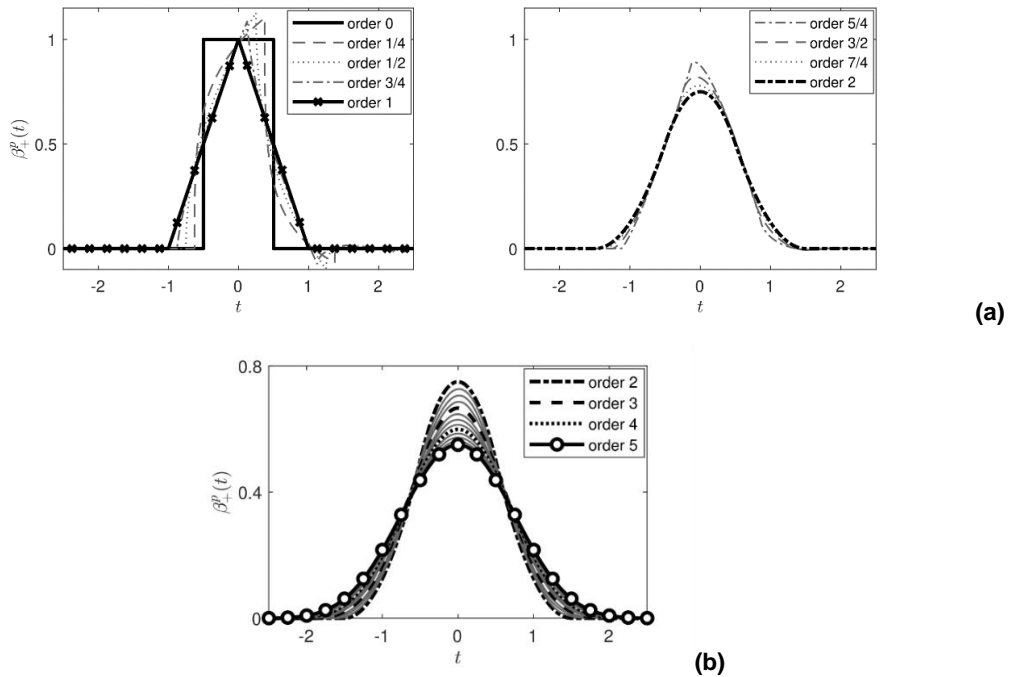


Fig. 5. (a) Centered B-spline of orders 0 to 2. (b) Centered B-splines for  $2 \leq p \leq 5$ .

The B-splines with fractional orders (0,1) were discarded because they have negative values. The partition of unity condition (4) is satisfied because the B-splines are scaling functions [29], and it is easily proved in the frequency domain

$$B_0^p\left(\frac{2\pi i}{\Delta}\right) = e^{-j\frac{2\pi i}{\Delta}\tau} \left(\frac{1-e^{-j\frac{2\pi i}{\Delta}\tau}}{j\frac{2\pi i}{\Delta}}\right)^{p+1} \quad (17)$$

the last quotient is 0 for any  $i \neq 0$ , and is 1 to  $i = 0$ . Then

$$B_0^p\left(\frac{2\pi i}{\Delta}\right) = e^{-j\pi(p+1)i} \delta[i] \quad (18)$$

All fractional and positive B-splines satisfy the mapping conditions of the QSP quantizer. Figure 6 shows the Fourier transform of positive splines of order 0 and 2. A feature of the NSD quantizer is not possible to make the error and the input statistically independent, although certain moments of the error can be independent [6]. In a probabilistic quantizer, the  $m^{th}$  conditional moment of the given error signal, is defined as

$$\mathbb{E}(\epsilon^m|x) = \int_{-\infty}^{+\infty} \epsilon^m h(\epsilon) \uparrow\uparrow\uparrow_{\Delta}(\epsilon+x)d\epsilon \quad (19)$$

where  $\uparrow\uparrow\uparrow_{\Delta}(x)$  is a Dirac comb of period  $\Delta$ . The conditional moment is functionally independent of the input  $x$  for  $m \geq 1$  if and only if [28, Theorem 7]

$$\frac{d^m H}{d\omega^m}\left(\frac{2\pi k}{\Delta}\right) = 0 \quad k = \pm 1, \pm 2, \dots \quad (20)$$

The  $m^{th}$  derivative of the Fourier transform of centered B-spline ([FTb-spline]) can be expressed as

$$\frac{d^m B_0^p(\omega)}{d\omega^m} = \frac{d^{m-1}}{d\omega^{m-1}}\left(\frac{dB_0^p(\omega)}{d\omega}\right) \quad (21)$$

with  $m \leq p$  because the B-spline of degree  $p$  are  $p$ -differentiable. To analyze the previous  $m^{th}$  derivative, we first obtain the first derivative.

$$\begin{aligned} \frac{d}{d\omega} \left\{ e^{-j\omega\tau} \left(\frac{1-e^{-j\omega\Delta}}{j\omega\Delta}\right)^{p+1} \right\} &= \frac{(p+1)}{\omega} e^{-j\omega\tau} \times \\ &\left(\frac{1-e^{-j\omega\Delta}}{j\omega\Delta}\right)^p \left[ e^{-j\omega\Delta} - \frac{1-e^{-j\omega\Delta}}{j\omega\Delta} \right] \\ &- j\tau e^{-j\omega\tau} \left(\frac{1-e^{-j\omega\Delta}}{j\omega\Delta}\right)^{p+1} \end{aligned} \quad (22)$$

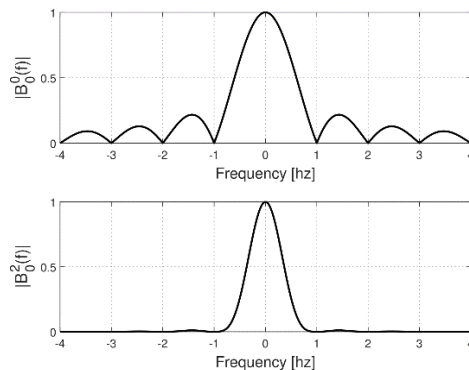


Fig. 6. Fourier transform magnitude of B-splines centered to orders 0 (uniform distribution) and 2.

Expressing in terms of  $B_+^0$  we have

$$\frac{dB_+^p(\omega)}{d\omega} = \frac{(p+1)}{\omega} e^{-j\omega\tau} \{B_+^{0p}(\omega)[e^{-j\omega\Delta} - B_+^0(\omega)] - j\tau B_+^{0p+1}(\omega)\}. \quad (23)$$

Since we are deriving a power function, the function will appear in every derivative, so we focus on this:

$$B_+^0(\omega)|_{\omega=\frac{2\pi i}{\Delta}} = \frac{1-e^{-j\omega\Delta}}{j\omega\Delta}|_{\omega=\frac{2\pi i}{\Delta}} = 0 \quad (24)$$

Therefore, the Fourier transform of the B-spline both centered and non-centered, satisfies the condition (20). Figure 7 shows the conditional moments of the error (19) for a B-spline of order 2 (see Figure 5(a)), which matches the results obtained by 2RPDF (Two Rectangular Probability Density Function) NSD quantizer generated from the sum of two statistically independent zero-mean uniformly distributed random variables, studied by Wannamaker et al. [6]. Notice that the first and second moments are constant; therefore, they are independent of the input, whereas the third moment is variable. Hence, the moments greater than the order of the B-spline ( $p > 2$ ) will continue to be variable and remain dependent on the input.

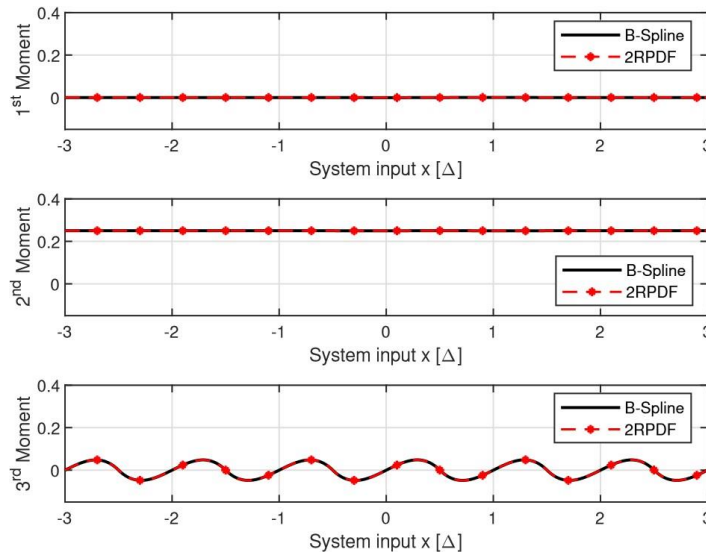


**Fig. 7.** Conditional moments of the error for a probabilistic quantizer using centered B-spline of order 2 vs 2RPDF.

### III. RESULTS

To observe the performance of the probabilistic quantizer, first a 1 Khz sinusoidal, shown in Figure 8, is used as input; and the centered B-spline of order 2 (see Figure 5a) is used as

mapping  $h$  in the quantizer. The discrete random variable  $w \in \mathbb{Z}$  is generated with probabilities  $p_k = h(x - k\Delta)$ , and the quantized output  $y$  is given by  $w\Delta$ . Note that this relation is input dependent. To generate  $w$ , we use the inversion method [35], which consists in obtaining the partial sums  $s_k = \sum_{i \leq k} p_i$  and generating only one uniform  $[0,1]$  random variable  $v$ . The sum can be seen as a monotone transformation, then  $p(s_k \leq v \leq s_{k+1}) = s_{k+1} - s_k = p_k$ . To obtain the output, we must generate a realization of  $v$ , and then quantize the input equal to  $k\Delta$ , where  $k$  is obtained from  $s_k \leq v \leq s_{k+1}$ . This can be done with any input and the code for all simulations is available online (GitHub repository [https://github.com/jphoyos/bspline\\_mapping](https://github.com/jphoyos/bspline_mapping)).

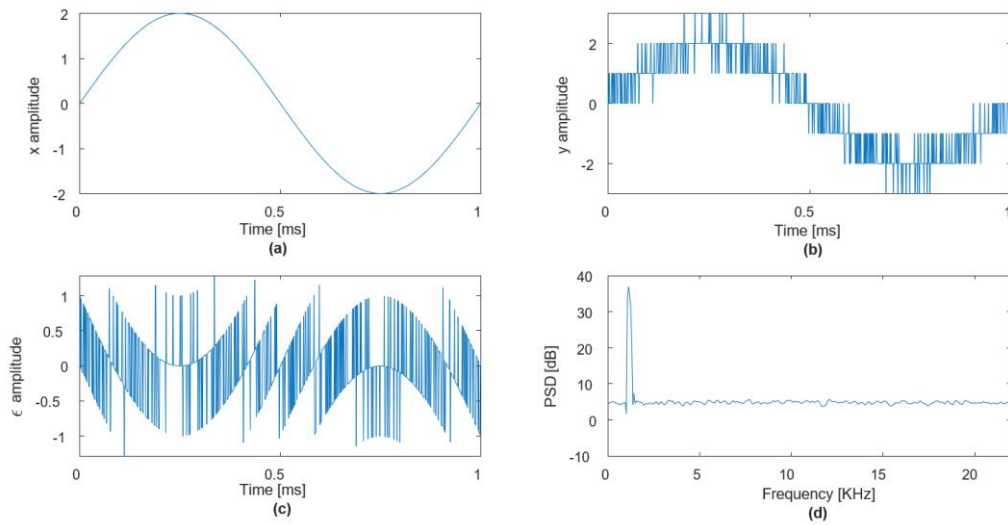


**Fig. 8.** Simulation quantization of a 1 KHz sine wave of 4.0 LSB peak-to-peak amplitude using probabilistic quantizer with centered spline of order 2. (a) Input signal  $x$  (b) output signal  $y$  (c) error signal  $\epsilon$ , and (d) power spectral density of the output signal.

As the order the spline is 2, only the first and second moment of the error are independent of the input (Figure 7). Hence, vestiges of the input signal are visible in the error signal Figure 8(c), as in the output signal Figure 8(b). The power spectral density shown in Figure 8(d) presents no distortion and suggests that the error is spectrally white. Our results are the same as those obtained by [7], but in our mappings we only needed to generate one random variable to do the quantization with the B-spline mapping and obtained the same performance. Also, to analyze the Rate-Distortion

$$R(D) = \min_{P_{Y|X} \in \mathcal{P}(X,D)} I(X,Y) \quad (25)$$

where  $\mathcal{P}(X, D)$  is the set of  $P_{Y|X}$  that satisfy  $\mathbb{E}[d(X, Y)] \leq D$ , we obtained the upper bounds on  $R(D)$  by evaluating the mutual information  $I(X, Y)$  for a specific  $Y$  and distortion  $D$ . Figure 9 presents the rate-distortion of the proposed mappings in the probabilistic quantizer and the standard Dither quantizer for a standard unit variance scalar Gaussian source. We used the mean square error distortion as measure  $d$  for each quantizer, guaranteeing that the distribution is on the interval  $[-\Delta/2, \Delta/2]$ .

The probabilistic quantizer with B-spline of order 0 obtains the same performance as the traditional Dither quantizer with uniform distribution, while the B-spline of order 1 and 3 obtain a rate equal to a Dither quantizer with Gaussian distribution. Conversely, with the fractional order, the worst performance is obtained due to the anti-symmetric distribution.

Then, the best rate was obtained by the B-spline of order 3 and the standard Dither quantizer with a Gaussian distribution, which renders all moments of the error independent of the system input; unfortunately, achieving it is complex because it would be necessary to generate and add theoretically infinite independent random variables [6]. Using a probabilistic quantizer with B-splines of order  $p \geq 3$ , the same rate is obtained and such complexity disappears since only one random variable is required to generate the distribution, rendering the  $p$  moments of the quantization error.

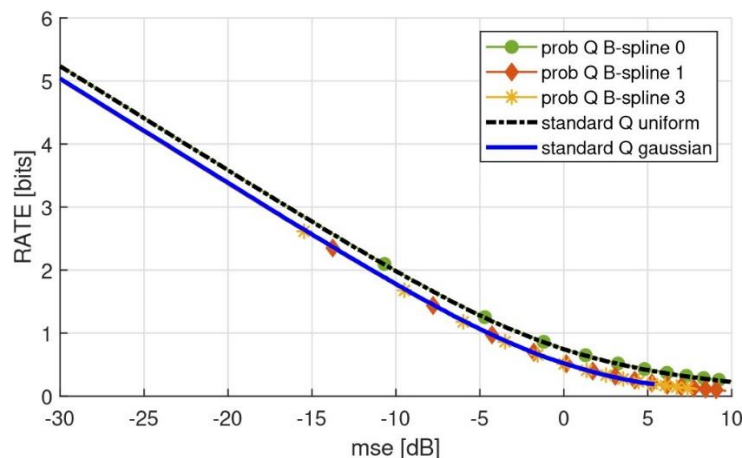


Fig. 9. Rate of the probabilistic quantizer with B-spline of order 0,1,3 and fractional 1.3 for a Gaussian source as compared to the standard NSD quantizer with uniform and Gaussian distribution.

#### IV. CONCLUSIONS

This paper proves that the centered positive B-splines fulfill all the necessary conditions to be mappings in a probabilistic quantizer. We show that the use of B-splines as mappings brings mathematical advantages because they can be explicitly characterized, thus

facilitating their analysis as well as that of the conditional moments of the error. This explicit characterization eliminates convergence issues that may arise with other mapping techniques. Furthermore, we established a meaningful relationship between the order of B-splines and the rendering of conditional moments of the error. This finding provides valuable insights to optimize the quantization process and achieve higher performance. Additionally, it is noteworthy that the implementation of B-splines as mappings requires generating a single random variable, which simplifies the overall system complexity. Finally, through extensive numerical experimentation, we validated the effectiveness of the probabilistic quantizer utilizing B-splines. Our experimental results have shown that this approach achieves performance on par with the NSD quantizer, a well-established benchmark. This result reinforces the practical feasibility and usefulness of employing B-splines in the quantization process.

#### AUTHORS' CONTRIBUTION

**Juan-Pablo Hoyos-Sanchez:** research; methodology; writing-original draft.

**Pablo-Emilio Jojoa:** supervision; methodology; writing-review and editing.

#### ACKNOWLEDGMENT

The authors thank the Ministry of Science, Technology and Innovation (MINCIENCIAS) of Colombia (811 of 2018), the Universidad Nacional de Colombia (Hermes Project No. 55818 and 61237), and the Universidad del Cauca.

#### REFERENCES

- [1] R. M. Gray, D. L. Neuhoff, "Quantization," *IEEE Transactions Information Theory*, vol. 44, no. 6, pp. 2325-2383, 1998. <https://doi.org/10.1109/18.720541>
- [2] B. Widrow, I. Kollar, *Quantization Noise: Roundoff Error in Digital Computation, Signal Processing, Control, and Communications*. Cambridge University Press, 2008. <https://doi.org/10.1017/cbo9780511754661>
- [3] S. P. Lipshitz, R. A. Wannamaker, J. Vanderkooy, "Quantization and Dither: A theoretical survey," *Journal of the Audio Engineering Society*, vol. 40, no. 5, pp. 355-375, 1992.
- [4] E. Akyol, K. Rose, "Nonuniform Dithered Quantization," in *Data Compression Conference*, 2009, pp. 435-435. <https://doi.org/10.1109/dcc.2009.78>
- [5] E. Akyol, K. Rose, "On Constrained Randomized Quantization," *IEEE Transactions Signal Processing*, vol. 61, no. 13, pp. 3291-3302, 2013. <https://doi.org/10.1109/tsp.2013.2261296>
- [6] R. A. Wannamaker, S. P. Lipshitz, J. Vanderkooy, J. N. Wright, "A theory of nonsubtractive Dither," *IEEE Transactions Signal Processing*, vol. 48, no. 2, pp. 499-516, 2000. <https://doi.org/10.1109/78.823976>
- [7] R. A. Wannamaker, "The theory of Dithered quantization," Doctoral Dissertation, University of Waterloo, Ontario, Canada, 1997.

## Positive B-splines used as Mappings in the Probabilistic Quantizer

- [8] L. Yue, P. Ganesan, B. S. Sathish, C. Manikandan, A. Niranjana, V. Elamaran, A. F. Hussein, "The importance of Dithering technique revisited with biomedical images-a survey," *IEEE Access*, vol. 7, pp. 3627-3634, 2019. <https://doi.org/10.1109/access.2018.2888503>
- [9] H. Pan, A. Abidi, "Spectral spurs due to quantization in nyquist adcs," *IEEE Transactions Circuits Systems I*, vol. 51, no. 8, pp. 1422-1439, 2004. <https://doi.org/10.1109/tcsi.2004.832755>
- [10] L. He, L. Jin, J. Yang, F. Lin, L. Yao, X. Jiang, "Self-Dithering technique for high-resolution sar adc design," *IEEE Transactions Circuits Systems II*, vol. 62, no. 12, pp. 1124-1128, 2015. <https://doi.org/10.1109/tcsii.2015.2468921>
- [11] T. Miki, N. Miura, H. Sonoda, K. Mizuta, M. Nagata, "A random interrupt Dithering sar technique for secure adc against reference-charge side-channel attack," *IEEE Transactions Circuits Systems II*, vol. 67, no. 1, pp. 14-18, 2020. <https://doi.org/10.1109/tcsii.2019.2901534>
- [12] H. Mo, X. Tan, M. P. Kennedy, "Maximizing the fundamental period of a Dithered digital delta-sigma modulator with constant input," in *Proceedings IEEE ICECS*, 2016, pp. 472-475. <https://doi.org/10.1109/icecs.2016.7841241>
- [13] H. Mo, M. P. Kennedy, "Masked Dithering of MASH Digital Delta-Sigma Modulators With Constant Inputs Using Multiple Linear Feedback Shift Registers," *IEEE Transactions Circuits Systems I*, vol. 64, no. 6, pp. 1390-1399, 2017. <https://doi.org/10.1109/tcsi.2017.2670365>
- [14] Y. Liao, X. Fan, Z. Hua, "Influence of lfsr Dither on the periods of a mash digital delta-sigma modulator," *IEEE Transactions Circuits Systems II*, vol. 66, no. 1, pp. 66-70, 2019. <https://doi.org/10.1109/tcsii.2018.2828600>
- [15] M. S. Fu, O. C. Au, "Data hiding in ordered Dithered halftone images," *Circuits Systems Signal Process*, vol. 20, pp. 209-232, 2001. <https://doi.org/10.1007/bf01201139>
- [16] J. Rapp, R. M. A. Dawson, V. K. Goyal, "Improving Lidar Depth Resolution with Dither," in *Proceedings IEEE ICIP*, 2018, pp. 1553-1557. <https://doi.org/10.1109/icip.2018.8451528>
- [17] E. T. Mbitu, S.-C. Chen, "Designing limit-cycle suppressor using Dithering and dual-input describing function methods," *Mathematics*, vol. 8, no. 11, e1978, 2020. <https://doi.org/10.3390/math8111978>
- [18] V. K. Goyal, J. Kovacevic, J. A. Kelner, "Quantized Frame Expansions with Erasures," *Applied and Computational Harmonic Analysis*, vol. 10, no. 3, pp. 203-233, 2001. <https://doi.org/10.1006/acha.2000.0340>
- [19] S. Rangan, V. K. Goyal, "Recursive consistent estimation with bounded noise," *IEEE Transaction Information Theory*, vol. 47, no. 1, pp. 457-464, 2001. <https://doi.org/10.1109/18.904562>
- [20] B. G. Bodmann, S. P. Lipshitz, "Randomly Dithered quantization and sigma-delta noise shaping for finite frames," *Applied and Computational Harmonic Analysis*, vol. 25, no. 3, pp. 367-380, 2008. <https://doi.org/10.1016/j.acha.2007.12.003>
- [21] P. T. Boufounos, "Universal Rate-Efficient Scalar Quantization," *IEEE Transactions Information Theory*, vol. 58, no. 3, pp. 1861-1872, 2012. <https://doi.org/10.1109/tit.2011.2173899>
- [22] C. Xu, V. Schellekens, L. Jacques, "Taking the Edge off Quantization: Projected Back Projection in Dithered Compressive Sensing," in *Proceedings IEEE SSP*, 2018, pp. 203-207. <https://doi.org/10.1109/ssp.2018.8450784>
- [23] L. Jacques, V. Cambareri, "Time for Dithering: fast and quantized random embeddings via the restricted isometry property," *Information and Inference: A Journal of the IMA*, vol. 6, no. 4, pp. 441-476, 2017. <https://doi.org/10.1093/imaiai/iax004>

- [24] A. Parada-Mayorga, D. L. Lau, J. H. Giraldo, G. R. Arce, "Blue-Noise sampling on graphs," *IEEE Transactions Signal Information Processing*, vol. 5, no. 3, pp. 554-569, 2019. <https://doi.org/10.1109/tsipn.2019.2922852>
- [25] A. Sanyal, N. Sun, "A simple and efficient Dithering method for vector quantizer based mismatch-shaped DACs," in *Proceedings IEEE ISCAS*, 2012, pp. 528-531. <https://doi.org/10.1109/iscas.2012.6272082>
- [26] N. West, G. Scheets, "Increasing the resolution of a uniform quantizer using a deterministic Dithering signal," in *Proceedings IEEE AUTOTESTCON*, 2012, pp. 54-57. <https://doi.org/10.1109/autest.2012.6334521>
- [27] R. Hadad, U. Erez, "Dithered Quantization via Orthogonal Transformations," *IEEE Transactions Signal Processing*, vol. 64, no. 22, pp. 5887-5900, 2016. <https://doi.org/10.1109/tsp.2016.2599482>
- [28] Y. C. Eldar, "Quantum signal processing," Doctora Dissertation, Massachusetts Institute of Technology, 2001.
- [29] M. Unser, T. Blu, "Wavelet theory demystified," *IEEE Transactions Signal Processing*, vol. 51, no. 2, pp. 470-483, 2003. <https://doi.org/10.1109/tsp.2002.807000>
- [30] M. Unser, A. Aldroubi, M. Eden, "A family of polynomial spline wavelet transforms," *Signal Processing*, vol. 30, no. 2, pp. 141-162, 1993. [https://doi.org/10.1016/0165-1684\(93\)90144-y](https://doi.org/10.1016/0165-1684(93)90144-y)
- [31] G. Makkena, M. B. Srinivas, "Nonlinear sequence transformation based continuous-time wavelet filter approximation," *Circuits, Systems, and Signal Processing*, vol. 37, no. 3, p. 965-983, 2018. <https://doi.org/10.1007/s00034-017-0591-9>
- [32] P. Noras, N. Aghazadeh, "Directional schemes for edge detection based on b-spline wavelets," *Circuits, Systems, and Signal Processing*, vol. 37, pp. 3973-3994, 2018. <https://doi.org/10.1007/s00034-018-0753-4>
- [33] M. A. Unser, "Ten good reasons for using spline wavelets," in *Wavelet Applications in Signal and Image Processing V*, A. Aldroubi, A. F. Laine, M. A. Unser, Eds., vol. 3169, International Society for Optics and Photonics. SPIE, 1997, pp. 422-431. <https://doi.org/10.1117/12.292801>
- [34] M. Unser, T. Blu, "Fractional splines and wavelets," *SIAM Review*, vol. 42, no. 1, pp. 43-67, 2000. <https://doi.org/10.1137/s0036144598349435>
- [35] L. Devroye, *Non-Uniform Random Variate Generation*, Springer New York, 1986. <https://doi.org/10.1007/978-1-4613-8643-8>



**Available in:**

<https://www.redalyc.org/articulo.oa?id=413982266001>

How to cite

Complete issue

More information about this article

Journal's webpage in redalyc.org

Scientific Information System Redalyc  
Diamond Open Access scientific journal network  
Non-commercial open infrastructure owned by academia

Juan-Pablo Hoyos-Sánchez, Pablo-Emilio Jojoa  
**Positive B-splines used as Mappings in the Probabilistic Quantizer**  
**B-Splines positivas usadas como mapeos en el cuantificador probabilístico**  
**B-Splines positivos usados como mapeamentos no cuantificador probabilístico**

*Revista Facultad de Ingeniería*  
vol. 33, no. 68, e17387, 2024  
Universidad Pedagógica y Tecnológica de Colombia,  
**ISSN:** 0121-1129  
**ISSN-E:** 2357-5328

**DOI:** <https://doi.org/10.19053/01211129.v33.n68.2024.17387>